Comprehensive Structural Study of Glassy and Metastable Crystalline $BaTi_2O_5$

Jianding Yu,*[,†] Shinji Kohara,[‡] Keiji Itoh,[§] Shunsuke Nozawa,[||] Satoru Miyoshi,[⊥] Yasutomo Arai,[†] Atsunobu Masuno,[#] Hiroki Taniguchi,[▽] Mitsuru Itoh,[▽] Masaki Takata,[‡] Toshiharu Fukunaga,[§] Shin-ya Koshihara,[||] Yoshihiro Kuroiwa,[‡,⊥] and Shinichi Yoda[†]

ISS Science Project Office, Japan Aerospace Exploration Agency, Tsukuba 305-8505, Japan, Research & Utilization Division, Japan Synchrotron Radiation Research Institute, Hyogo 679-5198, Japan, Research Reactor Institute, Kyoto University, Osaka 590-0494, Japan, Non-equilibrium Dynamics Project, Japan Science and Technology Agency, Tsukuba 305-0801, Japan, Graduate School of Science, Hiroshima University, Higashi-hiroshima 739-8526, Japan, Institute of Industrial Science, The University of Tokyo, Tokyo 153-8505, Japan, and Materials and Structures Laboratory, Tokyo Institute of Technology, Yokohama 226-8503, Japan

Received September 12, 2008. Revised Manuscript Received November 14, 2008

The structures of glassy and metastable crystalline $BaTi_2O_5$ fabricated by the containerless method were comprehensively investigated by combined X-ray and neutron diffractions, XANES analyses, and computer simulations. The three-dimensional atomic structure of glassy $BaTi_2O_5$ (g-$BaTi_2O_5$), simulated by Reverse Monte Carlo (RMC) modeling on diffraction data, shows that extremely distorted TiO_5 polyhedra interconnected with both corner- and edge-shared oxygen formed a higher packing density structure than that of conventional silicate glass linked with only corner-sharing of SiO_4 polyhedra. In addition, XANES measurement revealed that five-coordinated TiO_5 polyhedra were formable in the crystallized metastable α- and β-$BaTi_2O_5$ phases. The structure of metastable β-$BaTi_2O_5$ was solved by ab initio calculation, and refined by Rietveld refinement as group *Pnma* with unit lattices $a = 10.23784(4)$ Å, $b = 3.92715(1)$ Å, $c = 10.92757(4)$ Å. Our results show that the glass-forming ability enhanced by containerless processing, not by "strong glass former", fabricated new bulk oxide glasses with novel structures and properties.

Introduction

It is well-known that TiO_2 is one of the most important components in the electrical materials such as $BaTiO_3$, $PbTiO_3$. TiO_2 is also a desired component to enhance refractive index, because TiO_2 has a refractive index and a wavelength dispersion higher than those of diamond. Glass refractive index (GRI) is one of fundamental parameters for evaluating the performance of optical materials, but it does not exceed 2 in conventional silicate glasses. According to the Gladstone−Dale relationship,[1] it is possible to enhance GRI over 2 in the alkali-earth titanium oxides with large amount of TiO_2. However, such materials cannot be formed as a bulk glass without adding any "strong glass former".[2] Containerless processing is attractive for fabricating high "fragile glass",[2] such as YAG[3] and Mg_2SiO_4,[4] which cannot be formed by conventional methods. We recently fabricated a 2 mm diameter glassy sphere of ferroelectric $BaTi_2O_5$ by containerless processing, which exhibits an unusually high dielectric response during crystallization[5] and a high GRI of 2.14. Furthermore, lanthanide elements can be doped into the glassy structure to enhance GRI to 2.24 and create strong upconversion luminescence (see the Supporting Information, Figure S1). The high GRI offered a new opportunity for developing some crucial optical component, such as solid immersion lens used in the readout of optical disk. It was reported that a 1 mm diameter diamond solid immersion lens with GRI of about 2.4 enables the storage capacity of Blu-ray disk up to 150 GB.[6]

The bulk glassy $BaTi_2O_5$ (g-$BaTi_2O_5$) becomes not only an excellent practical material but also a unique model material for studying the structure of titanate glass without adding any strong glass former. Although numerous studies on the structure of titanium silicate glass have been carried out,[7−11] there is no report on the bulk silica-free high TiO_2 concentration glass, because of the inability of forming a bulk glass using conventional techniques. Furthermore, most early studies on titanium silicate glass have focused on four-coordinated TiO_4 and six-coordinated TiO_6, two common

* Corresponding author. E-mail: yo.kentei@jaxa.jp.
† Japan Aerospace Exploration Agency.
‡ Japan Synchrotron Radiation Research Institute.
§ Kyoto University.
|| Japan Science and Technology Agency.
⊥ Hiroshima University.
The University of Tokyo.
▽ Tokyo Institute of Technology.

(1) Mandarino, J. A. *Can. Mineral.* **1976**, *14*, 498.
(2) Angell, C. A. *Science* **1995**, *267*, 1924.
(3) Weber, J. K. R.; Felten, J. J.; Cho, B.; Nordine, P. C. *Nature* **1998**, *393*, 769.
(4) Kohara, S.; Suzuya, K.; Takeuchi, K.; Loong, C.-K.; Grimsditch, M.; Weber, J. K. R.; Tangeman, J. A.; Key, T. S. *Science* **2004**, *303*, 1649.
(5) Yu, J.; Arai, Y.; Masaki, T.; Ishikawa, T.; Yoda, S.; Kohara, S.; Taniguchi, H.; Itoh, M.; Kuroiwa, Y. *Chem. Mater.* **2006**, *18*, 2169.
(6) Shinoda, M.; Saito, K.; Kondo, T.; Nakaoki, A.; Furuki, M.; Takeda, M.; Yamamoto, M.; Schaich, T. J.; Oerle, B. M. v.; Godfried, H. P.; Kriele, P. A. C.; Houwman, E. P.; Nelissen, W. H. M.; Pels, G. J.; Spaaij, P. G. M. *Jpn. J. Appl. Phys.* **2006**, *45*, 1311.

10.1021/cm802483w CCC: $40.75 © 2009 American Chemical Society
Published on Web 12/29/2008

coordinations known as in crystalline titanate oxide. However, recently, the focus of attention has been changed to investigate unusual five-coordinated TiO_5 presented in the titanium silicate glass such as $Sr_2TiSi_2O_8$, $Ba_2TiSi_2O_8$, which are one of a few fresnoites containing five-coordinated TiO_5 and exhibiting piezoelectric and pyroelectric properties in the crystalline state. In our early study with X-ray diffraction measurments,[5] we have also revealed that the ferroelectric $BaTi_2O_5$ has a five-coordinated TiO_5 in glassy state. Although the formation of five-coordinated polyhedra was found in alminate and aluminosilicate glasses,[12] from the point view of the structural environment effects, the detail information of the short-range order (atomic configuration of TiO_5) and the intermediate-range order (interconnection of TiO_5) is necessary to interpret the optical properties such as the high GRI and the strong upconversion luminescence. The information of the structural difference between silicate titanium glass and silica-free titanate oxide glass is also expected for providing insight into the mechanism of glass forming without the "strong glass former". Furthermore, to obtain the glass-ceramics materials with tailored dielectric properties, the structural dependence between glassy and the crystalline $BaTi_2O_5$ must be revealed. Thus, we performed a comprehensive study combined the X-ray and neutron diffractions, X-ray absorption near edge structure (XANES) analysis, and structural modeling for g-$BaTi_2O_5$ and three crystallized phases (α-$BaTi_2O_5$, β-$BaTi_2O_5$, and γ-$BaTi_2O_5$).[5] Our results confirmed that TiO_5 polyhedra existed in the g-$BaTi_2O_5$ and two metastable phases (α-$BaTi_2O_5$ and β-$BaTi_2O_5$), and showed that the atomic configuration of TiO_5 and the intermediate-range order in g-$BaTi_2O_5$ is distinctly different from that of conventional titanium silicate glass.

Experimental Section

Structural Measurements. $BaTi_2O_5$ glass spheres were fabricated using containerless processing in an aerodynamic levitation furnace (ALF)[13,14] as described previouly.[5] To obtain the comprehensive structural information of $BaTi_2O_5$, we used X-ray diffraction, XANES, and neutron diffraction techniques. The X-ray diffraction experiments were performed at BL02B2 of SPring-8[15] for crystalline phases and BL04B2 of SPring-8[16] for bulk glassy sphere using 25 and 113 keV high-energy X-rays, respectively. The details of standard data analysis is described elsewhere.[15,16]

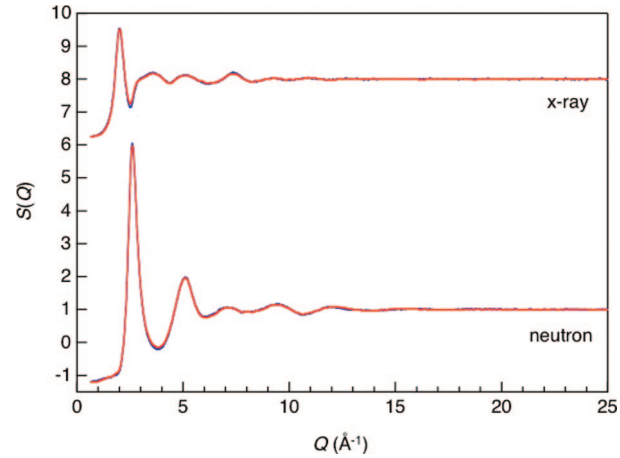

Figure 1. Total structure factors $S(Q)$ of g-$BaTi_2O_5$ (blue, experimental data; red, RMC simulation data). The differing features in the X-ray and neutron structure factors are due to the different scattering amplitudes of Ba, Ti, and O atoms and the different weighting factors between the two techniques.

The neutron diffraction measurement for glassy sphere was carried out in the HIT-II spectrometer installed at the pulsed neutron source in the High Energy Accelerator Research Organization. The glass sample was placed into a vanadium cell with an inner diameter of 8.0 mm and a thickness of 0.025 mm. The structure factor was derived by applying various corrections for the background, absorption and multiple scattering as well as normalization with a vanadium rod.[17]

The XANES spectra of Ti K-edge were collected in the transmission mode at the undulator beamline NW14A of the PF-AR. The incident X-ray was monochromatized using a Si(111) double-crystal monochromator with liquid-nitrogen cooling, and higher-order harmonics were removed with a harmonic-rejection mirror. The total energy resolution of the present apparatus was 1.0 eV at Ti K-edge. After the background fitted by a Victreen function was removed, all spectra were normalized for the average intensity of the spectral region from 5050 to 5200 eV.

Structural Simulation. Structure modeling of g-$BaTi_2O_5$ was performed by the Reverse Monte Carlo (RMC) simulation[18] on an ensemble of 4000, starting with a random configuration. Throughout the RMC simulation, the constraint of closest atom−atom approach was applied so as to avoid the appearance of unphysical spikes in the partial pair distribution functions. Furthermore, coordination number of oxygen around titanium was constrained to five. The atomic number density was chosen to 0.0695 $Å^{-3}$.

For solving the unknown structures of metastable crystals (α-$BaTi_2O_5$ and β-$BaTi_2O_5$), we performed an ab initio simulating using program of ENDEAVOU.[19] The structure parameters of β-phase were refined by Rietveld profile fitting and the electron-density distributions was calculated by maximum entropy method (MEM).[20]

Results and Discussions

Structure of g-$BaTi_2O_5$. Figure 1 shows the X-ray and neutron structure factors $S(Q)$ as functions of the wave vector of g-$BaTi_2O_5$ together with the results of RMC simulation. It is noted that the agreement between experimental data and

(7) Dingwell, D. B.; Paris, E.; Seifert, F.; Mottana, A.; Romano, C. *Phys. Chem. Miner.* **1994**, *21*, 501.
(8) Cormier, L.; Gaskell, P. H.; Calas, G.; Soper, A. K. *Phys. Rev. B* **1998**, *58*, 11322.
(9) Farges, F.; Brown, G. E. Jr.; Navrotsky, A.; Gan, H.; Rehr, J. J. *Geochim. Cosmochim. Acta* **1996**, *16*, 3039.
(10) Farges, F.; Brown, G. E. Jr.; Rehr, J. J. *Phys. Rev. B* **1997**, *56*, 1809.
(11) Yarker, C. A.; Johnson, A. V.; Wright, A. C.; Wong, J.; Greegor, R. B.; Lytle, W.; Sinclair, R. N. *J. Non-Cryst. Solids* **1986**, *79*, 117.
(12) Risbud, S. H.; Kirkpatrick, R. J.; Taglialvore, A. P.; Montez, B. *J. Am. Ceram. Soc.* **1987**, *70*, C10.
(13) Yu, J.; Paradis, P.-F.; Ishikawa, T.; Yoda, S. *Jpn. J. Appl. Phys* **2004**, *43*, 8135.
(14) Paradis, P.-F.; Babin, F.; Gagne, J.-M. *Rev. Sci. Instrum.* **1996**, *67*, 262.
(15) Nishibori, E.; Takata, M.; Kato, K.; Sakata, M.; Kubota, Y.; Aoyagi, S.; Kuroiwa, Y.; Yamakata, M.; Ikeda, N. *Nucl. Instrum. Methods Phys. Res., Sect. A* **2001**, *467−468*, 1045.
(16) Kohara, S.; Itou, M.; Suzuya, K.; Inamura, Y.; Sakurai, Y.; Ohishi, Y.; Takata, M. *J. Phys.: Condens. Matter* **2007**, *19*, 506101.
(17) Paalman, H. H.; Pings, C. J. *J. Appl. Phys.* **1962**, *33*, 2635.
(18) McGreevy, R. L. *J. Phys.: Condens. Matter* **2001**, *13*, R877.
(19) Putz, H.; Schön, J. C.; Jansen, M. *J. Appl. Crystallogr.* **1999**, *32*, 864.
(20) Tanaka, H.; Takata, M.; Nishibori, E.; Kato, K.; Iishi, T.; Sakata, M. *J. Appl. Crystallogr.* **2002**, *35*, 282.

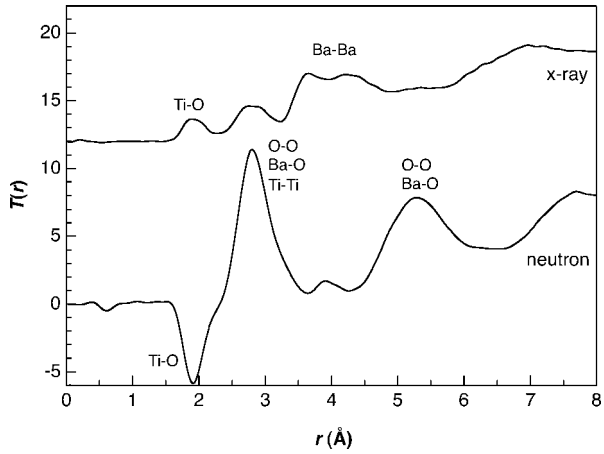

Figure 2. Total correlation functions $T(r)$ of g-$BaTi_2O_5$.

the RMC model is excellent. The Q position of the first sharp diffraction peaks are at 1.98 $Å^{-1}$ for X-rays and at 2.45 $Å^{-1}$ for neutrons. The neutron and X-ray data exhibit significant sensitivity differences in a wide range of wave vectors ($Q \approx 25$ $Å^{-1}$), and hence comprehensive computer simulations by RMC can be conducted to demonstrate the glass structure in terms of detailed spatial correlations among the constituent atoms and the geometry of the network unit.

The derived total correlation functions $T(r)$ are shown in Figure 2. The first peak in the $T(r)$ was assigned to the Ti−O bond length, which is 1.92 Å in g-$BaTi_2O_5$ as determined from a positive peak of X-ray diffraction and a negative peak of neutron diffraction. The negative peak is due to the negative neutron scattering length of Ti. Intriguingly, the peak is skewed toward the high r side, indicating a distribution of Ti−O distances from 1.60 to 2.50 Å due to highly distorted polyhedra. A fitting of the Ti−O peak using two Gaussian functions yielded two Ti−O correlation lengths at 1.91 and 2.13 Å, and the average coordination number N_{Ti-O} obtained is 4.87 ± 0.15 for X-ray data and 5.05 ± 0.15 for neutron data. In the case of alkali titanium silicate glass, TiO_5 polyhedra generally exhibit a square pyramid having one shorter Ti−O and four longer Ti−O bond.[8−11] In contrast to that, the partial pair distribution function $g_{ij}(r)$ of Ti−O derived from the RMC model (Figure 3), shows a prominent peak at 1.90 Å corresponding to four shorter Ti−O bonds and a small peak at 2.10−2.50 Å corresponding to one longer Ti−O bond. A strong peak at 2.80 Å in the neutron data demonstrates the correlation length of O−O. This peak also overlaps with both the Ba−O bond and Ti−Ti correlation peaks, according to the results of RMC simulation (Figure 3). A peak at approximately 4 Å is attributed to the contribution of the Ba−Ba correlation, consistent with that in glassy $BaSi_2O_5$.[21]

The $g_{ij}(r)$ of Ti−Ti pair shows a prominent peak at 2.9 Å for edge-sharing and a broad peak at approximately 3.5 Å for corner-sharing (Figure 3). These features suggested that TiO_5 polyhedra in g-$BaTi_2O_5$ are connected by both edge-

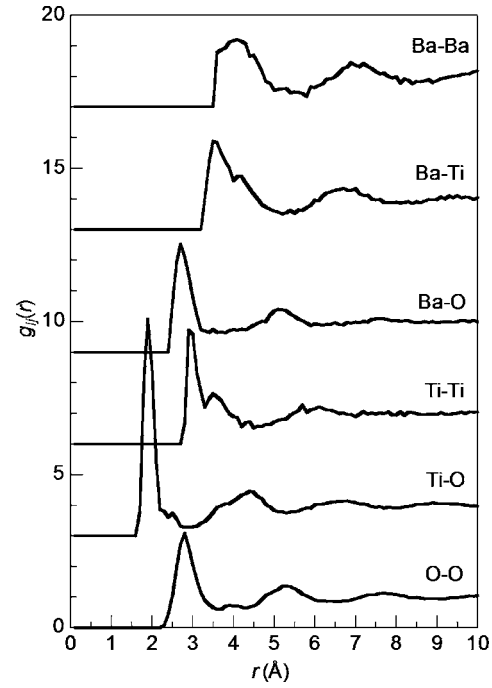

Figure 3. Partial pair correlation functions $g_{ij}(r)$ of g-$BaTi_2O_5$ computed by RMC simulation.

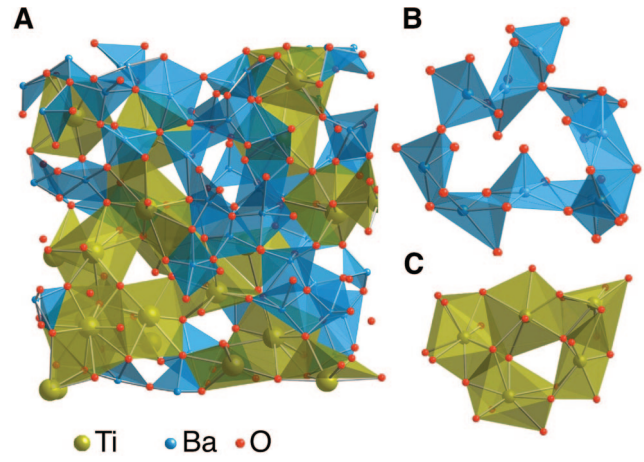

Figure 4. (a) Representation of the glass structure in a slice (20 Å × 20 Å × 10 Å) modeled by RMC simulation. (b) Network configuration of TiO_5 polyhedra linked by both edge-sharing and corner-sharing. (c) Network configuration of BaO_x ($x > 7$) polyhedra connected by edge-, face-, and vertex-sharing to form random dense packing.

and corner-shared oxygen. In generally, Ti−O polyhedra in titanium silicate glass is only connected by corner-sharing of oxygen with the Ti−Ti distance of 3.4 Å,[11] which implies that network structure in g-$BaTi_2O_5$ is different from that in titanium silicate glass.

To further illustrate the structural difference between g-$BaTi_2O_5$ and silica-free titanate glass, we analyzed the three-dimensional representation of the glassy structure, particularly the geometry of TiO_5 polyhedra and their connectivity in the glass state, from the RMC model. Figure 4a represents the distribution of Ti−O and Ba−O polyhedra obtained from the RMC configuration. Inhomogeneous distributions of Ti and Ba appear to exist within a space of 20 Å × 20 Å × 10 Å modeled by RMC simulation. Same tendency of forming the Ti-rich regions and Ba-rich regions was reported by the RMC simulation of a titanium-silicate

(21) Schlenz, H.; Kirfel, A.; Schulmeister, K.; Wartner, N.; Mader, W.; Raberg, W.; Wandelt, K.; Oligschleger, C.; Bender, S.; Franke, R.; Hormes, J.; Hoffbauer, W.; Lansmann, V.; Jansen, M.; Zotov, N.; Marian, C.; Putz, H.; Neuefeind, J. *J. Non-Cryst. Solids* **2002**, *297*, 37.

glass.[22] In the Ti-rich regions, distorted trigonal bipyramidal TiO_5 was connected by both edge- and corner-sharing to form network rings (Figure 4b). The Ti−O network is dominated by small rings with the following distribution: 3-fold rings (35%), 4-fold rings (25%), and 5-fold rings (20%). This distribution is similar to that of chalcogenide glass containing both corner- and edge-sharing,[23] and is in contrast to that of typical silicate glass linked by only corner-sharing SiO_4 tetrahedra.[24]

Figure 4c depicts the Ba polyhedra connected by edge-, face- and vertex-sharing to form a random dense packing. Associated with Ti polyhedra, the Ba polyhedra linkages included 3-fold rings (35%), 4-fold rings (22%), and 5-fold rings (15%). In addition, the average coordination number N_{Ba-O} in *g*-$BaTi_2O_5$ calculated using the RMC model is about 7.5, which is significantly higher than the 6 to 6.5 in barium silicate glass,[21] and nearly the same as the 8 in crystalline β-$BaTi_2O_5$. This feature implies that a high density packing of polyhedra are formed in *g*-$BaTi_2O_5$. The bond angle distribution of O−Ba−O also shows two peaks at 60 and 120° associated with a typical dense random packing.[25]

Metastable Structure. In the previous study,[5] we indicated three successive phase transitions, from glass to metastable α-phase and β-phase, and then to stable monoclinic γ-phase. The space group of γ-phase at room temperature has been confirmed by high-resolution X-ray powder diffraction as *C121,* consisted with the result for a single crystal.[26] However, the α- and β-phases could not be assigned to any known BaO-TiO_2 compounds. It is necessary to identify the structures of α- and β-phases for exploring the phase transition mechanisms and the anomalous dielectric behavior at phase transitions.[5] Therefore, an ab initio structure analysis from powder diffraction data was performed using the program of ENDEAVOU to identify the unknown structures. Before beginning ENDEAVOU, unit-cell parameters are needed to be calculated by indexing program from the peaks of X-ray powder diffraction patterns. For α-phase, because the lattice unit cell could not be determined unambiguously by the indexing program because of the insufficient number of X-ray diffraction peaks, TEM electron diffraction was performed to confirm the unit cell. The electron diffraction pattern as shown in Figure S2 in the Supporting Information suggested the α-phase having a hexagonal structure with $a = 6.6$ Å and $c = 11.1$ Å. However, the structural model of α-phase simulated by ENDEAVOU could not be refined conclusively by Rietveld profile fitting. The reason maybe mixed phases existed in the α-phase. For the β-phase, the lattice unit cell was assigned as having an orthorhombic structure, by both indexing program of ITO[27] and DICVOL9,[28] using more than 20 reflections. From the lattice parameters and X-ray diffraction data, a structural model with space group of *Pnma* was simulated by ENDEAVOU, and the structure parameters were refined by Rietveld profile fitting (Figure S3 in the Supporting Information), as shown in Table 1.

Table 1. Structural Parameters of β-$BaTi_2O_5$[a]

atoms	*x*	*y*	*z*	$U \times 10^2$ (Å^2)
Ba	0.05088(4)	1/4	0.82214(4)	0.756(5)
Ti1	0.2653(1)	1/4	0.1027(1)	0.59(3)
Ti2	0.1474(1)	1/4	0.4079(1)	0.53(3)
O1	0.0984(3)	1/4	0.0752(3)	0.6(1)
O2	0.8254(4)	1/4	0.5692(3)	0.6(1)
O3	0.4896(3)	1/4	0.1486(3)	0.6(1)
O4	0.2669(3)	1/4	0.2806(3)	0.4(1)
O5	0.1986(4)	1/4	0.5831(3)	0.2(1)

[a] These parameters were derived by refinement of the model for β-$BaTi_2O_5$ using powder X-ray data; space group *Pnma*, unit lattices $a = 10.23784(4)$ Å, $b = 3.92715(1)$ Å, $c = 10.92757(4)$ Å; *U*, isotropic.

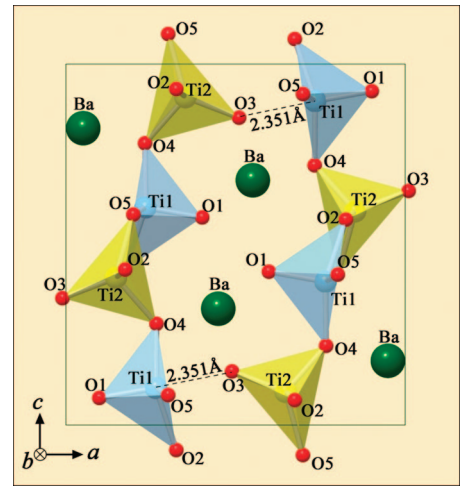

Figure 5. Projection of the crystal structure of β-$BaTi_2O_5$ onto the (010) plane. Two kinds of TiO_5 pyramidal polyhedra square-pyramid (aquamarine Ti1−O_5) and trigonal bipyramid (yellow Ti2−O_5) are shown. Both kinds of pyramid polyhedra are connected by edge-sharing (Ti−Ti = 3.0 Å) and corner-sharing (Ti−Ti = 3.5 Å) to form a two-dimensional layer parallel to the (100) plane. TiO_6 octahedra could be formed if unusually long Ti1−O3 bonds (2.35 Å) existed.

The analysis results of X-ray diffraction data show that Ti in the β-phase is located in two kinds of TiO_5 pyramidal polyhedra (Figure 5). One is a square pyramid (Ti1−O_5) and the other is a trigonal bipyramid (Ti2−O_5). Both pyramids have a short Ti═O bond (double bonded, about 1.73 Å) and four longer Ti−O bonds (from 1.85 to 2.00 Å). The two kinds of pyramidal polyhedra were connected by both corner- and edge-sharing to form a two-dimensional layer parallel to (100). The Ba−Ba pairs with the bonding lengths of 3.93 Å are located in the tunnels between two TiO_5 polyhedra layers. We noted that TiO_6 octahedra could be formed if we bond O3 to Ti1 to form an extremely long Ti1−O3 bond (2.35 Å). However, the electron-density distributions (Figure 6) calculated by MEM[20] indicated that the value of the minimum charge density at Ti1−O3 bond is 0.38 *e*/Å^3 within the background range, which is very lower than those of other Ti−O bonds (0.68−1.58 *e*/Å^3). Therefore, the Ti1−O3 bond is extremely weak and Ti ions are essentially coordinated by 5 oxygen atoms.

Ti−O Coordination of $BaTi_2O_5$. Information about the coordination geometry of the Ti site was investigated with

(22) Cormier, L.; Calas, G.; Gaskell, P. H. *J. Phys.: Condens. Matter* **1997**, *9*, 10129.
(23) Vashishta, P.; Kalia, R. K.; Antonio, G. A. *Phys. Rev. Lett.* **1989**, *62*, 1651.
(24) Kohara, S.; Suzuya, K. *J. Phys.: Condens. Matter* **2005**, *17*, S77.
(25) Howe, M. A.; McGreevy, R. L.; Pusztai, L.; Borzsák, I. *J. Mol. Liq.* **1993**, *25*, 205.
(26) Kimura, T.; Goto, T.; Yamane, H.; Iwata, H.; Kajiwara, T.; Akashi, T. *Acta Crystallogr., Sect. C* **2003**, *59*, i128.
(27) Ito, T. *Nature* **1949**, *164*, 755.
(28) Boultif, A.; Loueër, D. *J. Appl. Crystallogr.* **1991**, *24*, 98.

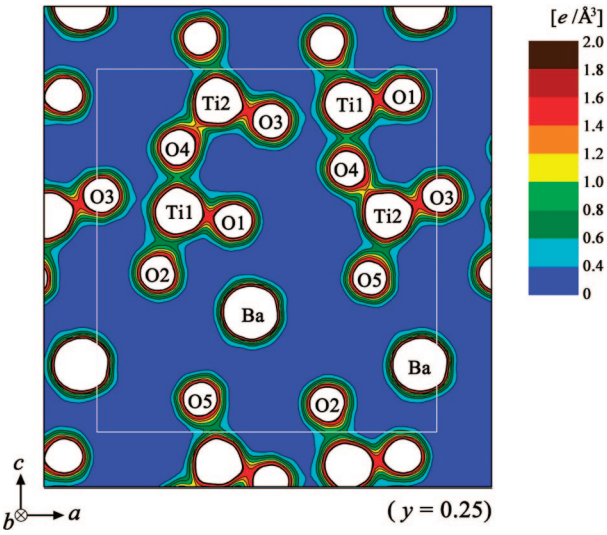

Figure 6. The electron-density distributions of β-$BaTi_2O_5$ phase in (040) plane calculated by maximum entropy method. The contours are drawn from 0.4 to 2.0 e/Å^3 with an interval of 0.2 e/Å^3.

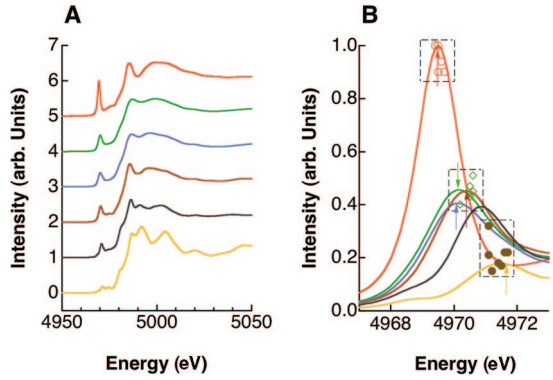

Figure 7. (a) Ti K-edge XANES spectra for glassy (g-) and three crystalline (α-, β-, γ-) $BaTi_2O_5$ phases, compared with Ti model compounds of four-coordinated α-Ba_2TiO_4 and six-coordinated R-TiO_2 (some of the curves have been displaced for clarity). (b) Detail of the normalized pre-edge feature; arrows show the positions of pre-edge peak. Three domains (surrounded by dotted-line squares) schematically illustrate four-, five-, and six-coordinated Ti (summarized from the data in ref 9) (red, α-Ba_2TiO_4; green, g-$BaTi_2O_5$; blue, α-$BaTi_2O_5$; brown, β-$BaTi_2O_5$; black, γ-$BaTi_2O_5$; yellow, R-TiO_2).

XANES measurement, which is sensitive to the coordination geometry of short-range order for selected elements. Figure 7a shows the Ti K-edge XANES spectra for glassy and crystalline $BaTi_2O_5$, compared with those of two reference model compounds of α-Ba_2TiO_4 with TiO_4 tetrahedra and rutile (R-TiO_2) with TiO_6 octahedra. The normalized pre-edge spectra are enlarged in Figure 7b to obtain information on Ti coordination from the pre-edge parameters. From the previous studies by Farges,[9,10] Ti coordination can be identify from the position of the normalized pre-edge that located at three well-separated domains corresponding to 4-, 5-, and 6-fold Ti coordination, as shown in Figure 7b. The pre-edge peaks of the reference model compounds of α-Ba_2TiO_4 and R-TiO_2 are located in the $^{[4]}$Ti and $^{[6]}$Ti domains, respectively, which is consistent with the results of the previous studies.[9,10] The pre-edge peaks of g-$BaTi_2O_5$ and metastable phases of α- and β-$BaTi_2O_5$ located all within the $^{[5]}$Ti domain. The prepeak of β-$BaTi_2O_5$ is at the center of the $^{[5]}$Ti domain, and those of g- and α-$BaTi_2O_5$ are shifted to the low-energy side of the domain, suggesting that β-$BaTi_2O_5$ has predominantly the $^{[5]}$Ti coordination, whereas g- and α-$BaTi_2O_5$ may include minor amounts of $^{[4]}$Ti. The peak of stable monoclinic γ-$BaTi_2O_5$, located at a position between $^{[5]}$Ti and $^{[6]}$Ti domains, implies the coexistence of $^{[5]}$Ti and $^{[6]}$Ti. It is possible that when we define the Ti−O bond distance using a cutoff of 2.3 Å, the structure shows that there are 1/3 the amount of $^{[5]}$Ti and 2/3 the amount of $^{[6]}$Ti coordination.

Conclusions

The structures of glassy and metastable crystalline $BaTi_2O_5$ fabricated by the containerless method were analyzed by combined X-ray and neutron diffraction analyses, XANES, and computer simulations. The intermediate-range structure of g-$BaTi_2O_5$ and the crystalline structure of metastable α- and β-$BaTi_2O_5$ were constructed of noncentrosymmetric TiO_5 polyhedra, which provides higher potential for yielding high dielectric constants than the structure of normal 4- or 6-coordinate Ti−O polyhedra. Same as in metastable crystalline β-$BaTi_2O_5$, TiO_5 polyhedra in g-$BaTi_2O_5$ interconnected with both corner- and edge-shared oxygen and formed a much higher dense random packing structure, which offered significant influence on the GRI and the upconversion effect.

Acknowledgment. We thank Professor Y. Kusano at Kurashiki University of Science and The Arts for measuring the electron diffraction data in Figure S2 of the Supporting Information.

Supporting Information Available: Three additional figures and crystallographic information file data (PDF). This material is available free of charge via the Internet at http://pubs.acs.org.

CM802483W